Resonance effects and quantum beats in attosecond transient absorption of helium

2014 J. Phys. B: At. Mol. Opt. Phys. 47 124009

(http://iopscience.iop.org/0953-4075/47/12/124009)

IOP Publishing Journal of Physics B: Atomic, Molecular and Optical Physics

J. Phys. B: At. Mol. Opt. Phys. **47** (2014) 124009 (8pp) doi:10.1088/0953-4075/47/12/124009

Resonance effects and quantum beats in attosecond transient absorption of helium

Michael Chini[1], **Xiaowei Wang**[1,2], **Yan Cheng**[1] **and Zenghu Chang**[1]

[1] Institute for the Frontier of Attosecond Science and Technology (iFAST), CREOL and Department of Physics, University of Central Florida, Orlando, FL 32816, USA
[2] Department of Physics, National University of Defense Technology, Changsha, Hunan 410073, People's Republic of China

E-mail: Zenghu.Chang@ucf.edu

Received 12 February 2014, revised 17 April 2014
Accepted for publication 23 April 2014
Published 10 June 2014

Abstract

We present theoretical simulations of the attosecond transient absorption of singly-excited states of helium atoms in the presence of a dressing near-infrared or infrared laser. In particular, we aim to address several unresolved questions in the transient absorption of helium and to resolve the remaining discrepancies between theory and experiment. We initially focus on the forklike structures in the Autler–Townes splitting of the 1s2p state and the effects of resonant coupling to the 1s2s and 1s3s states. We find that the delay-dependent features of the Autler–Townes doublet depend strongly on both the laser frequency detuning from resonance and on the laser pulse duration, and explain the lack of such structures in current experimental data. Next, we identify the interference mechanism which causes the half-cycle oscillations in the absorption spectrum below the excited state manifold. Finally, we observe for the first time the presence of quantum beating in the simulated transient absorption spectrogram, and discuss the conditions under which such wavepacket dynamics could be observed experimentally.

Keywords: attosecond, transient absorption, wavepacket dynamics

(Some figures may appear in colour only in the online journal)

1. Introduction

In recent years, the interaction of helium atoms with the combined fields of attosecond extreme ultraviolet (XUV) pulses and a femtosecond near-infrared (NIR) dressing laser field has attracted significant attention in the ultrafast laser community [1–3]. Recently, the attosecond electron interferometry technique [4, 5] has revealed the contributions of quantum path interferences and quantum beating to the two-colour multiphoton ionization process, resulting in fast oscillations in the electron yield. With the advent of attosecond transient absorption spectroscopy [6, 7], additional effects, such as sub-cycle ac Stark shifts [8, 9] and Autler–Townes splitting [10] of the excited state energy levels, as well as electromagnetically-induced transparency and the formation of light-induced states [11, 12] have been shown to play a significant role in the laser–atom interaction. In addition to these features, the quantum path interferences first observed in the photoelectron spectrum have been demonstrated in the transient absorption spectrogram both above and below the ionization threshold [12] with substantially higher fidelity allowed by the all-optical measurement.

As attosecond transient absorption spectroscopy is a relatively new technique, theoretical analyses have in general focused on relating a few major features of the transient absorption spectrogram to the dynamics of the excited electron, with interpretations guided by simplified model systems [7, 8, 10]. More recently, *ab initio* calculations in helium [11, 13] and neon [14] targets under the single active electron approximation as well as accurate calculations in more complex targets [15–17] have given excellent agreement with experiments and have aided in the interpretation of the delay-dependent absorption structures. In particular, recent calculations have revealed the origins of sub-cycle absorption oscillations in the vicinity of the ionization threshold of helium and the impact of ionization on the observation of

sub-cycle ac Stark shifts [13], the formation of the Autler–Townes doublet in the time domain [18] and the possibility of multiplet observation [10], the role of laser-induced phase shifts in the transient absorption line shape [19], and the impacts of temporal reshaping of the attosecond pulse in a dense gas target [20]. As the attosecond transient absorption measurement reveals the previously hidden dynamics of the bound electronic states, these simulations have served to enhance our understanding of previous measurements of ion yields [1, 2] and photoelectron spectra [5], helping to resolve discrepancies in the theoretical interpretation of these experiments [21] and placing the experiments on a unified theoretical foundation.

However, several unresolved questions remain in the comparison of the experimental and theoretical transient absorption spectra. For example, theory has predicted the presence of 'forklike' structures in the formation of the Autler–Townes doublet, with delay-dependent oscillations following the Rabi flopping frequency, rather than the dressing laser frequency [18]. However despite the availability of high-resolution measurements, such features have not been observed experimentally. Additionally, while quantum pathways responsible for the 'which-way' interference oscillations [13] in the vicinity of the helium ionization threshold have been identified, similar oscillations have been observed at energies below the excited state resonance manifold [12], which have so far not been addressed by theorists. Finally, transient absorption measurements and simulations have yet to reveal the presence of the 'quantum beats' resulting from the field-free evolution of the excited state wavepacket observed in photoelectron measurements, and in general the presence of relatively slowly varying features in experimentally-obtained transient absorption spectra has been ignored by both experimentalists and theorists. Here, we simulate the attosecond transient absorption of singly-excited states in helium atoms with the goal of resolving these remaining questions. By systematically varying the laser photon energy and selecting the sets of states which are allowed to interact, we break the transient absorption spectrogram down into various 'effects' which can be attributed to specific interactions.

2. Theoretical method

The theoretical method is based on solution of the time-dependent Schrödinger equation of the laser-dressed atom under the dipole approximation with one active electron, given (in atomic units) by:

$$\mathrm{i}\frac{\partial}{\partial t}\Psi(\boldsymbol{r},t) = [H_0 - \boldsymbol{r}\cdot\boldsymbol{F_X}(t-\tau_D) - \boldsymbol{r}\cdot\boldsymbol{F_L}(t)]\Psi(\boldsymbol{r},t), \quad (1)$$

where $\Psi(\boldsymbol{r},t)$ is the electron wavefunction and H_0 is the Hamiltonian of the field-free atom. The XUV and NIR laser fields, $\boldsymbol{F_X}(t)$ and $\boldsymbol{F_L}(t)$, are chosen to be Gaussian pulses, except where otherwise noted, characterized in terms of their respective amplitudes $F_{X,0}$ and $F_{L,0}$, carrier frequencies ω_X and ω_L, and pulse durations τ_X and τ_L, as well as the arrival time of the peak of the XUV pulse (time delay) τ_D. The NIR pulse arrives at time zero. When the two pulses are polarized along the z-axis, we can rewrite the time-dependent Hamiltonian in terms of the field-free Hamiltonian H_0 and the interaction Hamiltonian $H'(t)$:

$$H(t) = H_0 + H'(t), \quad (2)$$

where $H'(t) = -zF_L(t) - zF_X(t-\tau_D)$ describes the interaction of the atom with both laser fields. The electron wavefunction can be expanded on the set of stationary states of the field-free atom $\psi_j(\boldsymbol{r})$, for which $H_0\psi_j(\boldsymbol{r}) = E_j\psi_j(\boldsymbol{r})$ (here the jth state is specified by the principal and orbital angular momentum quantum numbers n and l). The wavefunction can then be written as $\Psi(\boldsymbol{r},t) = \sum_j c_j(t)\psi_j(\boldsymbol{r})$, where $c_j(t)$ is the jth state amplitude, and equation (1) can be rewritten:

$$\mathrm{i}\frac{\partial}{\partial t}\sum_j c_j(t)\psi_j(\boldsymbol{r}) = \sum_j [E_j - zF_L(t) - zF_X(t-\tau_D)] \times c_j(t)\psi_j(\boldsymbol{r}). \quad (3)$$

Projecting onto the state $\psi_a(\boldsymbol{r})$ in the set of $\psi_j(\boldsymbol{r})$ and using the definitions of the dipole matrix element $d_{aj} = \langle\psi_a|z|\psi_j\rangle$ for $j \neq a$ and of orthogonality $\langle\psi_a|\psi_j\rangle = \delta_{aj}$, we obtain the set of coupled differential equations for the state amplitudes:

$$\mathrm{i}\dot{c}_a = E_a c_a(t) - \sum_{j\neq a} d_{aj}[F_L(t) + F_X(t-\tau_D)]c_j(t), \quad (4)$$

which can be solved numerically using tabulated theoretical values of energies and dipole matrix elements [22] to obtain the time-dependent amplitudes and the full wavefunction. In total, sixteen bound states were used (1sns up to $n = 4$, 1snp up to $n = 7$, 1snd up to $n = 8$) due to the availability of tabulated dipole matrix elements. In our case, we solve the set of sixteen coupled equations (4) for each delay using a fourth-order Runge–Kutta differential equation solver in LabVIEW software.

The complex spectrum of the pulse transmitted through a thin target can then be obtained from the Beer–Lambert law as:

$$\tilde{\varepsilon}_{\mathrm{out}}(\omega) = \tilde{\varepsilon}_{\mathrm{in}}(\omega)\exp\left\{\mathrm{i}\frac{2\pi\omega}{c}\frac{\tilde{P}(\omega)}{\tilde{\varepsilon}_{\mathrm{in}}(\omega)}\mathrm{NL}\right\}, \quad (5)$$

where $\tilde{P}(\omega)$ is the polarization spectrum, given by the Fourier transform of the time-dependent dipole moment

$$P(t) = \langle\Psi(\boldsymbol{r},t)|z|\Psi(\boldsymbol{r},t)\rangle \quad (6)$$

of the atom, $\tilde{\varepsilon}_{\mathrm{in}}(\omega) = \int_{-\infty}^{\infty}\mathrm{d}t[F_L(t) + F_X(t-\tau_D)]\,\mathrm{e}^{\mathrm{i}\omega t}$ is the complex spectrum of the combined laser fields, and NL is the density-length product. The absorbance is then given by:

$$A(\omega) = \ln\left(\frac{|\tilde{\varepsilon}_{\mathrm{out}}(\omega)|^2}{|\tilde{\varepsilon}_{\mathrm{in}}(\omega)|^2}\right) = \frac{4\pi\omega}{c}\Im\left[\frac{\tilde{P}(\omega)}{\tilde{\varepsilon}_{\mathrm{in}}(\omega)}\right]\mathrm{NL}, \quad (7)$$

where $\Im$ denotes the imaginary part. This straightforward formulation of the laser–atom interaction allows simulation of the attosecond transient absorption in atomic bound states, and can be easily extended to autoionizing states [7, 23]. Unlike current *ab initio* simulations, the calculations are easily accessible to experimentalists with typical desktop computers, and can be applied to a wide range of targets using existing spectroscopic data for energies and dipole matrix elements.

3. Resonance effects in Autler–Townes splitting

We investigate the forklike structure in the Autler–Townes splitting of the 1s2p state, first shown in calculations by Wu and coworkers [18]. The forklike structures appear as nested interference patterns between the main Autler–Townes doublet in the 1s2p absorption near zero delay, and were revealed in simulations of the transient absorption under the condition of resonant coupling of the 1s2p and 1s2s states. These features, which were attributed to Rabi oscillations in the population of the 1s2p state, were found to be a predominant feature in the transient absorption spectrogram when the resonance condition is perfectly met and when the Rabi frequency Ω is small in comparison to the laser frequency (that is, when the rotating wave approximation is valid). However, in previous experimental data [11, 12], the nested forklike features could not be resolved.

Two possible reasons for the lack of experimental observation of the forklike structures stem from the pulse parameters used in the calculations and experiments. First, Wu and coworkers chose the central photon energy of the dressing laser pulse to be perfectly resonant with the 1s2p→1s2s transition, while the experiments have used laser pulses with central wavelengths of 730 to 780 nm, near resonance with the 1s2p→1s3s and 1s2p→1s3d transitions. Because the nested forklike structures arise from Rabi oscillations, experimental observation may require the use of a dressing laser pulse which is perfectly resonant with only one transition, thus demanding dressing laser pulses with a central wavelength near 2 μm ($E_{2p}-E_{2s}=0.6$ eV). Additionally, while attosecond experiments are typically performed with few-cycle laser pulses, the calculations in [18] were performed with relatively long dressing laser pulses. For a few-cycle pulse, the pulse duration may become comparable to the Rabi oscillation period, thus obscuring the forklike structures. Furthermore, because few-cycle pulses must be composed from extremely broad spectral bandwidths, the conditions for resonance are not well defined.

In figure 1, we simulate the transient absorption spectrogram of helium in the vicinity of the 1s2p excited state (E_{2p} = 21.22 eV, relative to the energy level of the neutral ground state $E_{1s}=0$) as a function of the time delay τ_D between the attosecond pulse and the dressing laser under similar conditions as in the experiments of [12]. Negative delays indicate that the attosecond pulse arrives on the target before the dressing laser pulse. The dressing laser intensity had a full-width-at-half-maximum pulse duration of three optical cycles and a peak intensity of 5×10^{12} W cm^{-2}, while the attosecond pulse had a duration of 200 as, a central photon energy of 22.5 eV, and a peak intensity of 1×10^{10} W cm^{-2}. The dressing laser frequency was chosen to be near resonance with the 2p→3s transition (E_{3s} = 22.92 eV) with a Rabi frequency of ~0.6 eV. For simplicity, only the ground state, 2p, and 3s states were considered in the calculations. For a frequency detuning $\Delta = \omega_L - |E_{3s} - E_{2p}|$ equal to zero, we observe symmetric splitting of the 1s2p absorption line into two branches for small negative delays, consistent with the Autler–Townes splitting. When the laser frequency is detuned slightly from

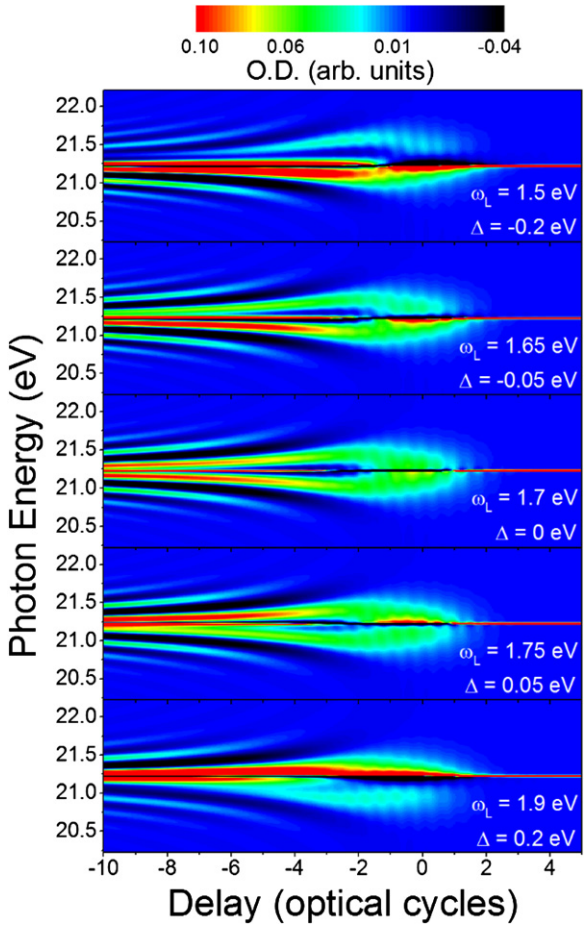

Figure 1. Delay-dependent absorption in the vicinity of the 1s2p excited states for near-resonant coupling to the 1s3s state ($E_{3s} - E_{2p} = 1.7$ eV). While the characteristic energy level splitting can be seen for all detunings, the predicted forklike structure is limited to the main Autler–Townes doublet even when the resonance condition is perfectly met.

resonance, the splitting remains, but is no longer symmetric. However, even when the resonance condition is met perfectly (centre panel), the forklike structure is limited to the primary Autler–Townes doublet and the nested interferences are absent.

In figure 2, we again simulate the transient absorption in the vicinity of the 1s2p state, but here we consider the resonant coupling to the 1s2s state (E_{2s} = 20.62 eV). Due to the larger dipole matrix element between the 2p and 2s energy levels, the dressing laser intensity was reduced to 7×10^{11} W cm^{-2} to maintain the same Rabi oscillation frequency as in figure 1. Here, however, the pulse duration of the three-cycle dressing laser pulse (~20.67 fs) is nearly three times longer than in figure 1 due to the longer wavelength. When the frequency detuning of the laser is zero, we clearly observe the nested forklike features within the Autler–Townes doublet, in good agreement with previous calculations with relatively longer pulses [18]. Furthermore, we find that the Rabi oscillation dynamics survive even when the resonance condition is not perfectly met, provided that the detuning from resonance is relatively small ($\Delta \leqslant 0.15$ eV).

In both figures 1 and 2, the pulse duration was fixed to three optical cycles. In the case of the 0.6 eV dressing laser

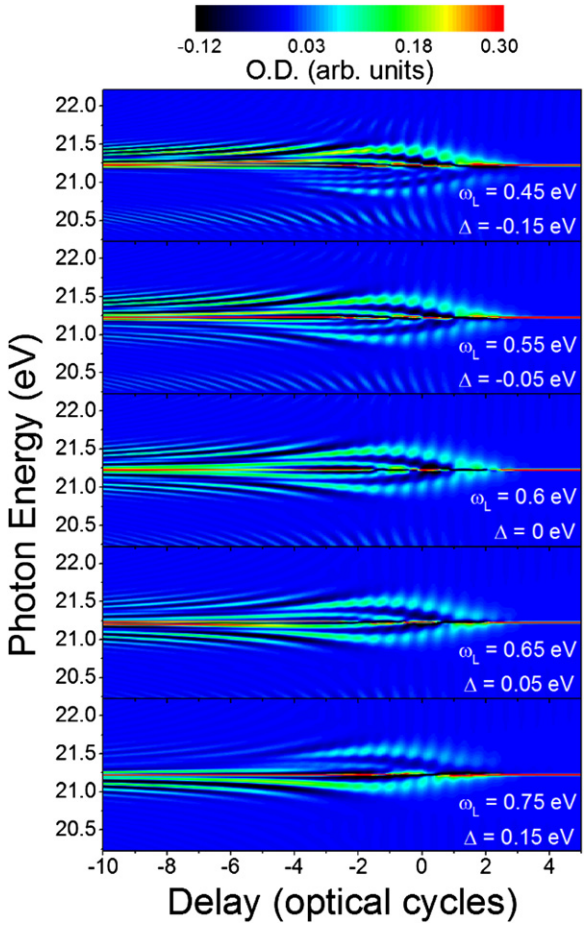

Figure 2. Delay-dependent absorption in the vicinity of the 1s2p excited states for near-resonant coupling to the 1s2s state ($E_{2p} - E_{2s} = 0.6$ eV). The nested forklike structures can be observed for small detuning, but weaken as the laser frequency moves away from resonance.

field, this corresponds to a pulse duration of ∼20.7 fs, much longer than the Rabi cycle period of ∼6.9 fs. On the other hand, for the 1.7 eV dressing laser frequency, the pulse duration of ∼7.3 fs is comparable to the Rabi period. Therefore, it is likely that the Rabi oscillations are obscured by the few-cycle pulse durations used in experiments, rather than the small energy detuning. In figure 3, we simulate the transient absorption under the same conditions as in the third panel of figure 1 ($\omega_L = 1.7$ eV, $\Delta = 0$), but using a dressing laser pulse duration of 10 cycles (∼24.3 fs). Here, we find that the nested forklike structures return, indicating that experimental observation of such structures may not require the use of long-wavelength dressing laser sources, but can be achieved using relatively long dressing laser pulses from Ti:Sapphire lasers.

4. Quantum pathway and optical interferences

Next, we turn our attention to the oscillating spectral features below the helium excited state manifold. In figure 4(a), we plot the simulated transient absorption of helium (including all bound states) using a dressing laser with $\omega_L = 1.7$ eV, three cycles pulse duration, and peak intensity of 5×10^{12} W cm^{-2}. We observe oscillations in the delay-dependent spectrogram

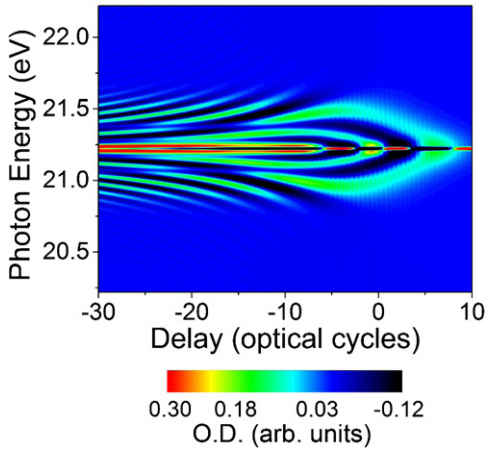

Figure 3. Delay-dependent absorption in the vicinity of the 1s2p excited states for resonant coupling to the 1s3s state ($E_{3s} - E_{2p} = \omega_L = 1.7$ eV), but with a relatively long (10 optical cycle FWHM) pulse duration. The nested forklike structures dominate the transient absorption spectrogram near zero delay.

which extend to large negative delays both near the ionization threshold (∼24 to 25 eV) and below the 1s2p excited state energy (∼19.5 to 20 eV). The features near the ionization threshold have been discussed in detail before [12–14], and have been attributed to quantum 'which-way' interference in the population of 1snp Rydberg states. In the quantum interference model, the oscillating features arise from the interference between a 'direct' pathway, which is populated by the XUV pulse alone, and an 'indirect' pathway, which is populated by a multiphoton process involving both the attosecond pulse and the dressing laser.

As illustrated in figure 5(a), two different pathways for excitation of an electron from the ground state with energy E_0 to the final state with energy E_f can be found: via absorption of an XUV photon with frequency $\omega_2 = E_f - E_0$, or via XUV excitation to the intermediate state with energy E_i (absorption of a photon with frequency $\omega_1 = E_i - E_0$) followed by the absorption of two NIR photons. For negative delays (XUV first), both paths are possible, and the interference of the two pathways leads to a delay dependence in the final state population after the interaction with both laser pulses depending on whether the two pathways add constructively or destructively. This process is known as 'which-way' interference, as the observer cannot determine which pathway is responsible for the excitation of the electron to the final state.

In transient absorption, it is more convenient to approach this problem in terms of the time-dependent dipole moment, given by equation (6), which yields the polarization spectrum. The initial excitation by the attosecond pulse ('direct' pathway) induces a coherence between the ground state and final state. This coherence begins to emit dipole radiation with frequency ω_2, which is phase-shifted by π with respect to the ω_2 frequency component of the attosecond pulse. In the absence of the NIR laser, the incident and emitted fields add destructively, resulting in the well-known Lorentzian absorption feature. Upon the arrival of the NIR pulse, the 'indirect' pathway can similarly induce a coherence which radiates at ω_2. Depending on the delay between the attosecond

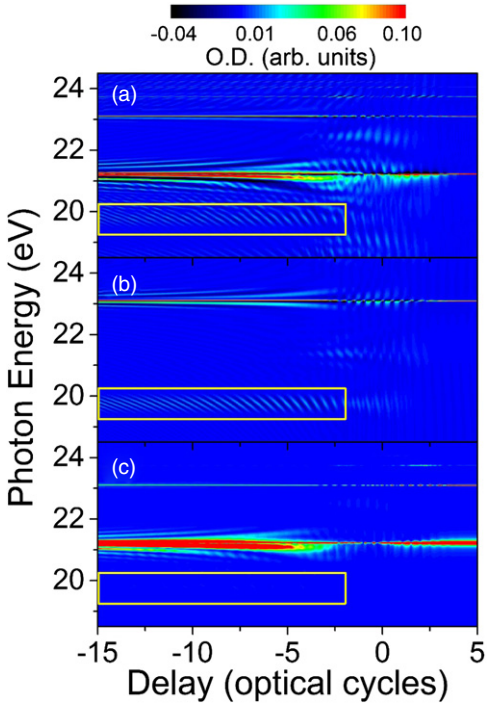

Figure 4. Interference in the delay-dependent absorption near 19.68 eV with a dressing laser frequency $\omega_L = 1.7$ eV. The full calculation in (a) includes the contributions from 16 bound states, and the half-cycle interference oscillations are indicated by the yellow box. In (b), the calculation has been repeated after removing the 1s2p, 1s4p, 1s5p, 1s6p, and 1s7p states. The presence of the interference oscillation near 19.68 eV suggests that it does not result from quantum 'which-way' interference, as no 'direct' pathway is possible. In (c) the power spectrum $|\tilde{P}(\omega)|^2$ of the atomic dipole radiation is plotted for the same conditions as in (a), with all states included. The lack of the interference oscillations indicates an optical interference mechanism, as explained in the text. While the emission feature near 19.7 eV is very weak and cannot be seen in the false colour plot of (c), it results in a measurable interference pattern when combined with the transmitted attosecond field.

pulse and the NIR laser field, these two contributions to the dipole radiation will interfere with one another (and with the incident field), which in turn can lead to delay-dependent oscillations with a frequency of $E_f - E_i \approx 2\omega_L$ in the measured absorption near ω_2. In the case of the observed delay-dependent oscillations at 24–25 eV in helium atoms [12, 13], coherences between the ground state and the high-lying 1snp states can be induced either 'directly' by the attosecond pulse or 'indirectly' via a three-photon (XUV + NIR + NIR) process wherein the attosecond pulse initially excites the 1s2p state. The 'which-way' interference is therefore imprinted on the transient absorption spectrum as an oscillation with frequency equal to $E_{n\mathrm{p}} - E_{2\mathrm{p}}$ in the vicinity of the 1s*n*p excited state absorption line. Importantly, these interferences can be observed not only in the transient absorption spectrum, but also in the delay-dependent polarization spectrum, which can in principle be observed experimentally by detecting the spectrum of the dipole emission perpendicular to the laser propagation direction.

Although the 'which-way' interference model can explain the transient absorption oscillations observed in the vicinity of the high-lying 1s*n*p states, it cannot explain the oscillations observed in the transient absorption near 19.7 eV. This low-energy absorption feature lies completely below the 1s*nl* excited state manifold, and there are no 1s*n*p excited states with this energy; therefore there is no 'direct' pathway for the 'which-way' interference to occur. While the photon energy of this feature suggests the involvement of the 1s3p state through a three-photon process analogous to the 'indirect' pathway ($E_{3\mathrm{p}} - 2\omega_L \approx 19.7$ eV), past experiments have indicated that removing either of the two pathways will quench the 'which-way' interference and destroy the oscillation features [14]. In figure 4(b), we remove the possibility of any other 'direct' pathway by removing all 1s*n*p states with the exception of 1s3p. We find that the strong oscillations remain both above and below the ionization threshold in spite of the presence of only one quantum pathway, suggesting that this feature results from another process.

To explain this, we propose that the observed interference does not arise from quantum 'which-way' interference, but instead results from an optical interference process involving the incident attosecond light and the laser-induced dipole emission. While the 'which-way' interference stems primarily from interfering components of the dipole emission resulting from the 'direct' and 'indirect' quantum pathways, we find that the delay-dependent oscillations near 19.7 eV stem from the interference between the attosecond pulse 'transmitted' by the medium and the dipole radiation 'emitted' by the dressed atom, as illustrated in figure 5(b). Here, there is only one possible pathway through which dipole radiation can be emitted with frequency ω_2, whereby the attosecond pulse initially excites the state with energy E_i, which then forms laser-induced sidebands in the presence of the NIR field with energies $E_i \pm m\omega_L$, where m is an integer. Due to parity conservation, only those sidebands with even m will radiate XUV light, and figure 5(b) shows only the sideband with $m = 2$, which radiates with frequency ω_2, for clarity. This dipole emission will then interfere with the component of the attosecond pulse with frequency ω_2, and the interference can be observed in the transient absorption. As the dipole emission near ω_2 can only arise from the combined action of the attosecond pulse and the dressing laser field, the 'emitted' field is delayed with respect to the 'transmitted' field, leading to alternating absorption and emission features as the interference changes from destructive to constructive with sub-optical-cycle periodicity. In the case of the helium transient absorption experiments, the delay-dependent oscillations observed near 19.7 eV result can be described as the interference between the transmitted attosecond spectrum and the polarization induced by the laser-dressed 1s3p state in the $m = -2$ sideband.

We can distinguish the features which arise due to the 'which-way' interference from the features which arise due to the optical interference by comparing the delay-dependent polarization spectrum $|\tilde{P}(\omega)|^2$ to the transient absorption spectrogram. Because the 'which-way' interference results from two interfering contributions to the polarization, it can be observed directly from the polarization spectrum. On the other hand, the optical interference can be observed only in the transient absorption spectrum, as it requires the

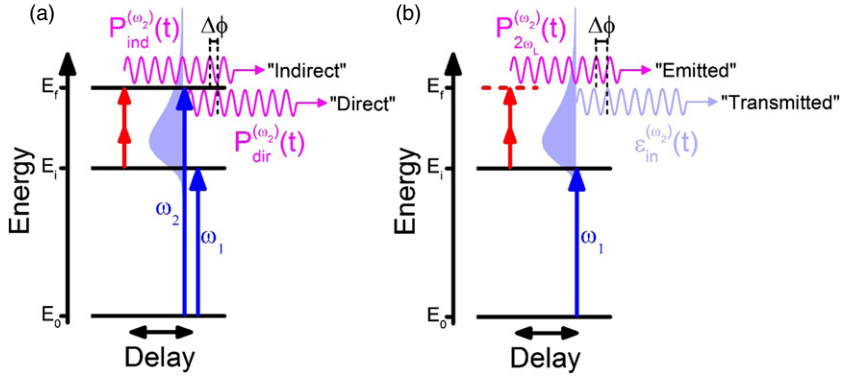

Figure 5. Comparison of 'which-way' and optical interference models. (a) In the 'which-way' interference, the final state can be excited both by the attosecond pulse alone ('direct') and by the combined attosecond and NIR laser fields ('indirect'). Each of these excitation pathways induces a time-dependent dipole, $P_{\rm dir}^{(\omega_2)}$ and $P_{\rm ind}^{(\omega_2)}$ respectively, which both oscillate with the frequency $\omega_2 = E_f - E_0$. Depending on the delay, these two components may add up constructively or destructively, leading to a modulation of the measured signal. (b) In the optical interference, there is no state with energy E_f, and therefore the component of the attosecond spectrum (pale blue shaded) with frequency ω_2 does not induce dipole emission on its own. When the NIR laser is present, the state with energy E_i forms sidebands resulting in the emission with frequency ω_2. This laser-induced dipole radiation ('emitted') will interfere with the 'transmitted' components of the attosecond spectrum with frequency ω_2, leading to a delay-dependent modulation in the measured signal. Blue arrows indicate atomic transitions initiated by the attosecond pulse (with spectrum indicated by the pale blue shaded area), while red arrows indicate transitions resulting from the NIR pulse. Magenta sinusoidal arrows indicate the dipole emission with frequency ω_2, while the pale blue sinusoidal arrow indicates the transmitted component of the attosecond spectrum.

transmitted components of the attosecond spectrum in addition to the dipole emission. In figure 4(c), we show the delay-dependent polarization spectrum, which can be compared to the transient absorption spectrum in figure 4(a). In particular, we find that those features in the transient absorption spectrum corresponding to electron wavepacket dynamics, such as the energy level splitting and quantum 'which-way' interferences in the vicinity of the 1s2p and 1s3p energy levels, are also present in the polarization spectrum. However, unlike the transient absorption, the delay-dependent polarization spectrum is found not to exhibit the sub-cycle oscillations near 19.7 eV. The absence of these oscillations suggests that they arise from the optical interference of the 'emitted' polarization and the 'transmitted' optical field, rather than from 'direct' and 'indirect' contributions to the polarization.

5. Quantum beats in attosecond transient absorption

Finally, we investigate the possibility of observing quantum beats in the transient absorption spectrogram. In previous photoelectron measurements [5], the quantum beats were attributed to electrons which were initially excited by the attosecond pulse to different 1s*n*p states, and subsequently ionized by the dressing laser pulse to the same final state in the continuum. The quantum beats therefore arise from the field-free evolution of the excited state wavepacket in the time interval between the two pulses. In the case of attosecond transient absorption, however, the final state is typically a bound state, and so the conditions for observing the quantum beating are somewhat different. Rather than observing the quantum beats in the absorption spectrum above the ionization threshold, we expect that the wavepacket motion may be imprinted as a slow variation on the absorption in the vicinity of the excited state energy levels. Here, we propose a mechanism by which the quantum beating of the 1s4p and higher-lying states can be observed in the transient absorption in the vicinity of the 1s2p absorption line. Because the bandwidth of the dressing infrared laser is large, the 1s4p and higher-lying states can be coupled to the 1s2p state through the emission of two photons within the spectrum of state-of-the-art few-cycle Ti:Sapphire lasers. For example, population initially excited to the 1s5p and 1s6p states can be transferred to the 1s2p state via stimulated emission of two 876 and 829 nm photons, respectively. In figure 6, we simulate the attosecond transient absorption of the 1s2p state coupled to the 1s5p and 1s6p states under the influence of a dressing laser with intensity of 5×10^{12} W cm^{-2} and a central energy of $\omega_L = 1.5$ eV. For simplicity, only the 2p, 3s, 5p, and 6p excited state energy levels were included in the calculation. Figure 6(a) shows the attosecond transient absorption spectrogram, which exhibits relatively slow oscillations with a superimposed half-cycle modulation. To guide the eye, we have also plotted a sinusoidal oscillation with a period equal to the quantum beat period of the 1s5p and 1s6p states, $T_{5p,6p} = 2\pi/|E_{6p} - E_{5p}| = 25.83$ fs, which is in good agreement with the slow oscillations on the high-energy side of the 1s2p resonance. In figure 6(b) we have integrated the absorbance spectrum within a small energy window (21.25 to 21.28 eV) just above the 1s2p resonance, and find that the quantum beat results in a strong modulation of the absorption in the vicinity of the 1s2p energy level. Such slow oscillations are clearly present in previous transient absorption measurements, but unambiguous identification of the quantum beats will require measurements over a much larger range of negative delays.

Experimentally, however, it is not possible to remove unwanted states, and the contributions of the entire excited state manifold may obscure the quantum beats shown in figure 6. In figure 7, we compare the quantum beats of figure 6 with calculations including the full 16-state basis

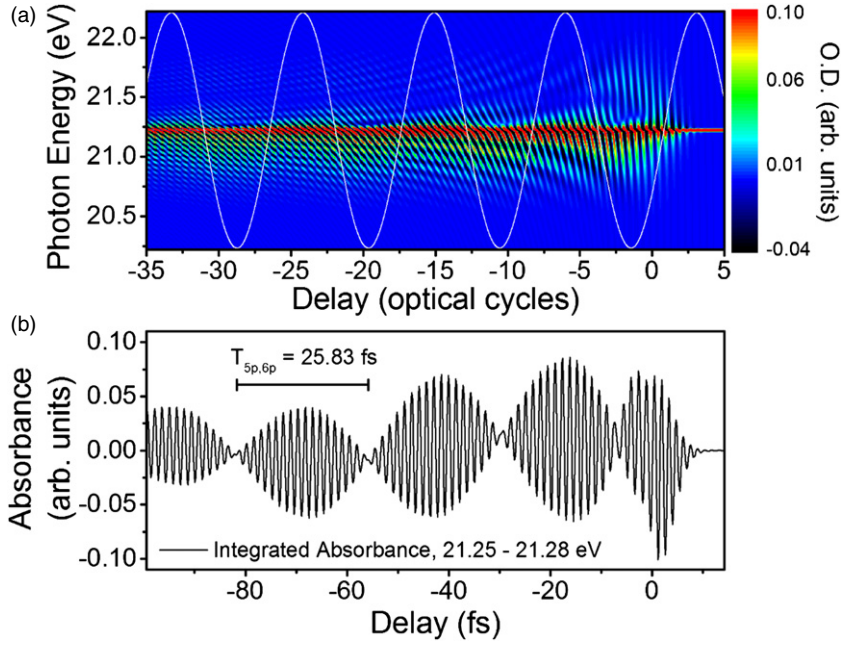

Figure 6. Quantum beats in the delay-dependent absorption near the 1s2p excited state with a reduced excited state basis set consisting of the 1s2p, 1s3s, 1s5p, and 1s6p states. Relatively slow oscillations are present on the high-energy side of the 1s2p absorption line in (a) with periodicity equal to that of the quantum beating of the 1s5p and 1s6p state (white curve). The integrated absorbance from 21.25 to 21.28 eV in (b) clearly shows the quantum beat effect with a periodicity of 25.83 fs.

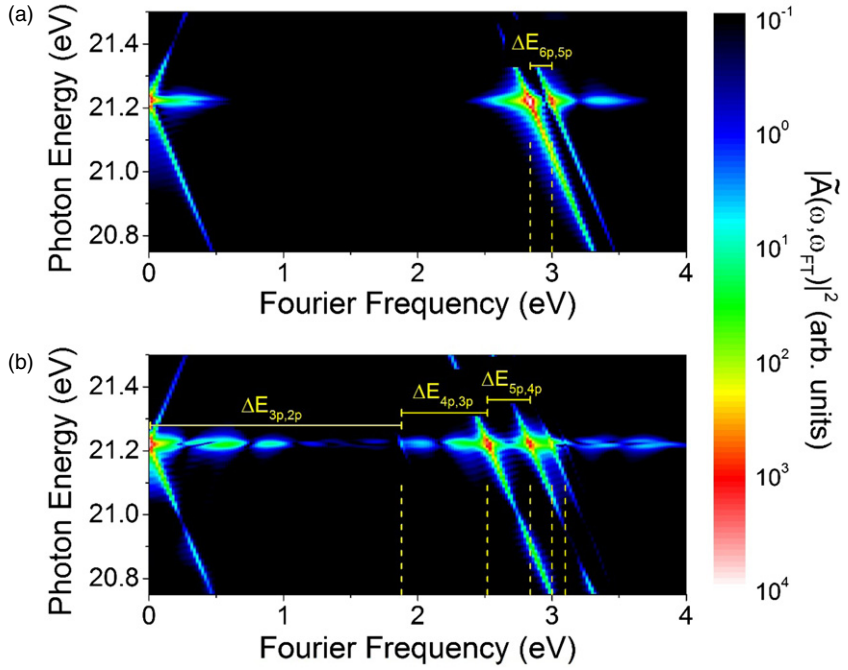

Figure 7. Fourier transform analysis of the quantum beats in the vicinity of the 1s2p excited state. (a) For the reduced basis set (same as in figure 6), the dominant quantum beat arises from the 1s5p and 1s6p states. (b) When the full 16-state basis set is used, additional beat frequencies corresponding to each of the 1snp energy level differences $\Delta E_{n'\mathrm{p},n\mathrm{p}} = E_{n'\mathrm{p}} - E_{n\mathrm{p}}$ can be observed.

set. By taking the Fourier transform of the delay-dependent absorbance, we can identify the quantum beat frequencies as 'sidebands' of the half-cycle oscillations. This is clear in figure 7(a), where the sidebands are separated by 0.16 eV, which is equal to the energy difference between the 1s5p and 1s6p states. Comparing figures 7(a) and (b), we find that the inclusion of the full basis set results in the appearance of additional peaks in the energy-dependent Fourier spectrum, with separations equal to the various excited state energy level differences as indicated. However, because the exact energy of the sideband beaks varies with the photon energy, integration over a narrow energy region is necessary to extract the quantum beat frequencies.

Because clear observation of the quantum beat requires sufficient population to be transferred from the higher-lying 1s*n*p states to the 1s2p state, in the calculations of figures 6

and 7 we have intentionally modified the attosecond pulse spectrum, so that the spectrum in the vicinity of the 1s5p and 1s6p states is ∼10 times stronger than in the vicinity of the 1s2p state. This was done by multiplying the Gaussian spectrum centred at 22.5 eV by a step function:

$$f(\omega) = \begin{cases} 1, \omega \leqslant 23.5 \text{ eV} \\ 10, \omega > 23.5 \text{ eV} \end{cases}. \quad (8)$$

Without this modification, only the 1s4p and 1s5p beat frequencies can be clearly identified in the Fourier analysis when all states are included. Experimental observation of multiple quantum beats can therefore be achieved by modifying the spectrum of the attosecond pulse using suitable foil filters [14], as has previously been demonstrated in attosecond transient absorption, or by using multilayer XUV mirrors [24, 25], and requires an XUV spectrometer with high energy resolution [26, 27].

6. Conclusion

In conclusion, by simulating the response of helium atoms to an isolated attosecond pulse and delayed dressing laser field, we have addressed several unresolved questions in the attosecond transient absorption of helium. In particular, we find that the observation of the forklike structure in the Autler–Townes splitting of the 1s2p state requires the use of relatively long dressing laser pulses, which can be achieved by using few-cycle pulses in the mid-infrared or by using many-cycle pulses at Ti:Sapphire wavelengths. Furthermore, we demonstrate that the sub-cycle oscillations below the 1s*n*p excited state manifold observed in experiments results not from quantum 'which-way' interference, as has previously been shown to yield similar structures in photoelectron measurements, but from optical interference between the 'transmitted' attosecond pulse and the 'emitted' polarization field of the laser-dressed atom. Finally, we propose a method by which the quantum beats arising from the excited state wavepacket evolution can be experimentally observed in the transient absorption measurement. By cataloguing these effects and addressing several remaining questions in attosecond transient absorption, these results will aid in the extension of attosecond transient absorption spectroscopy to more complicated targets, such as molecules [28] and condensed matter [29].

Acknowledgments

This work is funded by the DARPA PULSE program by a grant from AMRDEC, the National Science Foundation and the Army Research Office.

References

[1] Johnsson P *et al* 2005 *Phys. Rev. Lett.* **95** 013001
[2] Ranitovic P *et al* 2010 *New J. Phys.* **12** 013008
[3] Holler M, Schapper F, Gallmann L and Keller U 2011 *Phys. Rev. Lett.* **106** 123601
[4] Choi N N, Jiang T F, Morishita T, Lee M H and Lin C D 2010 *Phys. Rev.* A **82** 013409
[5] Mauritsson J *et al* 2010 *Phys. Rev. Lett.* **105** 053001
[6] Goulielmakis E *et al* 2010 *Nature* **466** 739
[7] Wang H, Chini M, Chen S, Zhang C, He F, Cheng Y, Wu Y, Thumm U and Chang Z 2010 *Phys. Rev. Lett.* **105** 143002
[8] Chini M, Zhao B, Wang H, Cheng Y, Hu S X and Chang Z 2012 *Phys. Rev. Lett.* **109** 073601
[9] Wirth A *et al* 2011 *Science* **334** 195–200
[10] Pfeiffer A N and Leone S R 2012 *Phys. Rev.* A **85** 053422
[11] Chen S, Bell M J, Beck A R, Mashiko H, Wu M, Pfeiffer A N, Gaarde M B, Neumark D M, Leone S R and Schafer K J 2012 *Phys. Rev.* A **86** 063408
[12] Chini M, Wang X, Cheng Y, Wu Y, Zhao D, Telnov D A, Chu S and Chang Z 2013 *Sci. Rep.* **3** 1105
[13] Chen S, Wu M, Gaarde M B and Schafer K J 2013 *Phys. Rev.* A **87** 033408
[14] Wang X, Chini M, Cheng Y, Wu Y, Tong X and Chang Z 2013 *Phys. Rev.* A **87** 063413
[15] Tarana M and Greene C H 2012 *Phys. Rev.* A **85** 013411
[16] Santra R, Yakovlev V S, Pfeifer T and Loh Z 2011 *Phys. Rev.* A **83** 033405
[17] Pabst S, Sytcheva A, Moulet A, Wirth A, Goulielmakis E and Santra R 2012 *Phys. Rev.* A **86** 063411
[18] Wu M, Chen S, Gaarde M B and Schafer K J 2013 *Phys. Rev.* A **88** 043416
[19] Chen S, Wu M, Gaarde M B and Schafer K J 2013 *Phys. Rev.* A **88** 033409
[20] Pfeiffer A N, Bell M J, Beck A R, Mashiko H, Neumark D M and Leone S R 2013 *Phys. Rev.* A **88** 051402
[21] Lucchini M, Herrmann J, Ludwig A, Locher R, Sabbar M, Gallmann L and Keller U 2013 *New J. Phys.* **15** 103010
[22] Drake G W F 2006 *Springer Handbook of Atomic, Molecular, and Optical Physics* (New York: Springer) pp 199–219
[23] Ott C, Kaldun A, Raith P, Meyer K, Laux M, Zhang Y, Hagstotz S, Ding T, Heck R and Pfeifer T 2012 arXiv:1205.0519
[24] Morlens A, Balcou P, Zeitoun P, Valentin C, Laude V and Kazamias S 2005 *Opt. Lett.* **30** 1554–6
[25] Hofstetter M *et al* 2011 *Opt. Express* **19** 1767–76
[26] Wang X, Chini M, Cheng Y, Wu Y and Chang Z 2013 *Appl. Opt.* **52** 323–9
[27] Ott C, Kaldun A, Raith P, Meyer K, Laux M, Evers J, Keitel C H, Greene C H and Pfeifer T 2013 *Science* **340** 716–20
[28] Sansone G, Reduzzi M, Dubrouil A, Feng C, Nisoli M, Calegari F, Lin C D, Chu W C, Poletto L and Frassetto F 2013 *Conf. on Lasers and Electro Optics/Quantum Electronics and Laser Science (San Jose, CA)* QF2C.1
[29] Schultze M *et al* 2013 *Nature* **493** 75–8